

# **Secondary wave lift degradation**

**Pekka Koivisto**

# **Secondary wave lift degradation**

Pekka Koivisto, Aalto University

Finnish Transport Safety Agency  
Liikenteen turvallisuusvirasto Trafi  
Trafiksäkerhetsverket Trafi  
Helsinki Helsingfors 2015

ISBN 978-952-311-113-4  
ISSN 2342-0294 (verkkójulkaisu)

## **FOREWORD**

This research report is focused on the role of a secondary wave in lift degradation during simulated take-off for a wing section that has been applied with anti-icing fluid. It forms part of the third year studies in the Icing project initiated by the Finnish Transport Safety Agency, Trafi.

The research was performed by the team of Arteform Oy, headed by MSc Juha Kivekäs.

Helsinki, December 22nd 2015

Erkki Soinne

Chief Adviser, Aeronautics

Finnish Transport Safety Agency, Trafi

# Index

## Abstract

<b>1</b>	<b>Introduction .....</b>	<b>5</b>
<b>2</b>	<b>Test Arrangements.....</b>	<b>6</b>
	<b>2.1 Wind Tunnel .....</b>	<b>6</b>
	<b>2.2 Wind Tunnel Model.....</b>	<b>6</b>
<b>3</b>	<b>Data Acquisition and Assessment of Accuracy.....</b>	<b>7</b>
<b>4</b>	<b>Measurement Program .....</b>	<b>8</b>
<b>5.</b>	<b>Previous test results</b>	<b>10</b>
	<b>5.1 Clean wing aerodynamics</b>	<b>10</b>
	<b>5.2 General Qualitative Observations</b>	<b>10</b>
	<b>5.3 Lift Degradation Results .....</b>	<b>12</b>
<b>6.</b>	<b>The secondary wave tests .....</b>	<b>14</b>
	<b>6.1 General Qualitative Observations .....</b>	<b>14</b>
	<b>6.2 Lift degradation measurements.....</b>	<b>16</b>
<b>7.</b>	<b>Conclusions .....</b>	<b>17</b>
<b>8.</b>	<b>References .....</b>	<b>18</b>

## **ABSTRACT**

Secondary wave is a fluid wave appearing on the wing upper side immediately after the rotation of an anti-iced airliner during take-off. The existence of secondary waves has been frequently reported since the first studies of anti-icing fluid effects on the wing lift degradation. However studies on its contribution to the lift degradation after the rotation are scarce.

In this report the secondary wave is studied visually by video recordings and by lift force measurements during simulated take-offs in a wind tunnel. Two different configurations of a DLR-F15 wing section are utilized: slats and flaps extended and retracted. The mechanism of the emergence of a secondary wave is analyzed using video recordings and the contribution of it on the lift degradation is measured.

It appeared that the buildup mechanisms of secondary waves seem to be different for different wing section geometries and configurations. The contribution of the secondary wave on the lift degradation turned out to be very significant on the studied wing section.

# 1. Introduction

Present Aerodynamic Acceptance Test (AAT) for de/anti-icing fluids is defined in SAE Aerospace Standard AS 5900<sup>1</sup>. The flight tests and extensive wind tunnel tests that formed the scientific basis of AAT considers predominantly lift coefficient degradation caused by de/anti-icing fluids. The reasoning behind this is reviewed in detail in Ref. 2. Already in the early studies on de/anti-icing fluid tests during 1990's the role of the so called secondary waves on the lift degradation during lift-off were recognized<sup>3,4</sup>.

Secondary wave is a fluid wave appearing on the wing upper side immediately after the rotation of an airliner during take-off. Several studies<sup>3,4,5</sup> report evidence on secondary wave effect on lift degradation after rotation. However it's difficult to isolate quantitatively the contribution of the secondary wave effect from all the other fluid effects. Perhaps the most accurate estimate is reported by Broeren et al.<sup>5</sup> There is no visual evidence (photographic or videotape) of secondary wave in Ref 5 as the reasoning on its existence is done indirectly by measuring lift losses with the fluid applied and wiped out on different areas on the wing. The interconnection between the secondary wave and lift degradation is often reported only qualitatively as in the following quote from Runyan et al<sup>4</sup>: "Lift losses on the two-dimensional model with the flaps 15, gapped-slat configuration are shown in .... These losses are much larger than those for the flaps 5, sealed-slat configuration. Secondary fluid waves were observed at both flap settings on the two-dimensional model immediately after rotation, just as had been observed on the three dimensional half model. The secondary waves were, again, larger for the flaps 15 configuration than for the flaps 5 configuration." (the wing section considered is B-737-200ADV wing section at 75% span location)

In all of the studies referred above a secondary wave appeared. It should be noted that the wing section in Ref 5 did not have a slat at all whereas in Ref 4 there were both slotted slat and sealed slat configurations. In the present study a three element DLR-F15 wing section is used to study the effects of the secondary wave on the lift degradation. Also some visual analysis based on videotape recording is included. The configurations included in the tests are slats and flaps extended (11° and 15°) and retracted.

## 2. Test Arrangements

### 2.1 Wind Tunnel

Aalto University Low Speed Wind Tunnel is a closed circuit wind tunnel with an octagonal test section with dimensions of 2 m x 2 m and a test section length of 4 m. The flow uniformity in the test section is < 0.14 %, and turbulence level < 0.28 % at a wind tunnel speed of 60 m/s.

### 2.2 Wing Section Model

The tests of the present study were conducted with a two dimensional 3 element rotating model that was mounted to a three component balance to measure the aerodynamic lift, drag and pitching moment. The model was equipped with endplates to minimize the three dimensionality of the flow. Two dimensionality and absence of flow separations were confirmed by tufts. Slats and flaps were adjustable (Fig 1.) and so it was possible to simulate the real operational sequence of extending the flaps and slats just prior to the test.

The wing section model has the geometry of a DLR-F15 (Ref. 6) profile and a chord of 0.65 m. The model span was 1.5 m which implies an area of 0.975 m<sup>2</sup>. Anti-ice fluid was applied on the whole upper surface area during the tests (Fig 1.).



**Figure 1. Rotating wing section model in wind tunnel.**

### **3. Data Acquisition and Assessment of Accuracy**

There is a standard measuring software in the wind tunnel collecting the wind tunnel temperature, airspeed, dynamic pressure, relative humidity, balance forces and moments (lift, drag and pitching moment in this case) and wing angle of attack. For qualitative analysis of the fluid flow-off the test runs were videoed through a Plexiglas window on the ceiling of the test section.

The initial mean thicknesses of the fluid layers were measured directly from the containers used to apply the fluid and via point wise measurements of film thickness using an Elcometer type of thickness gauge. After subtracting the off dripped fluid before the test from the applied amount the two methods gave an initial thickness that agreed within 5%.

The maximum weight of the applied fluid on the measured lift values was less than 0.1 % of the lift force.

The effect of anti-icing treatments on the take-off performance was evaluated by measuring the lift coefficient degradation  $\Delta C_l$  due to the contamination. This means sequential  $C_l$  - measurements of a clean wing and a contaminated wing. As the result is a difference between the two lift coefficients at the same angle of attack the repeatability of the tests is more relevant than the absolute accuracy of the lift coefficient itself.

In Ref. 7 the effect of several anti-icing treatment related parameters were studied. The lift coefficient measurements for a clean wing gave in Ref. 7 well repeatable results at the fixed angle of attack of interest ( $8^\circ$ ). For 20 separate clean wing tests the lift coefficient mean value was 1.281 with a standard deviation of 0.0028, which gives a coefficient of variation of 0.219%. In case of anti-icing treatment the lift coefficient repeatability was not as good. Just after rotation at an angle of attack of  $8^\circ$  the standard deviation of lift coefficient for 2 to 4 runs with similar anti-icing treatment varied between 0.005 and 0.01. One of the reasons for this was the difficulty to repeat all the conditions of the fluid applications. In case of frost it was not possible to end up with two similar frost layers to define a repeatability.



## 4. Measurement Program

Considering wing contamination related performance degradation the most critical condition is the One Engine Inoperative (OEI) situation, in which the airliner is flying at the speed of  $V_2$  after lift-off up to the so called cleaning altitude at which the flaps and slats are retracted (>400 ft above ground level as per EASA CS 25.121<sup>8</sup>). As the performance degradation due to anti-icing treatment has practically diminished well before reaching the cleaning altitude the relevant phases of flight regarding performance degradation are take-off roll and initial climb at speed  $V_2$ .

While developing the Aerodynamic Acceptance Test (AAT), Hill and Zierter<sup>3</sup> evaluated five specific take-off performance criteria following FAR 25 requirements:

- Adequate margin between 1 g stall speed ( $V_{s1g}$ ) and take-off safety speed  $V_2$
- Adequate margin between minimum unstick and lift-off speed
- Adequate aft body-runway clearance during take-off
- Adequate take-off acceleration and climb capabilities
- Adequate maneuver capability to stall warning

Hill and Zierter<sup>3</sup> determined that the most critical of these five criteria was maintaining adequate margin between the 1 g stall speed and  $V_2$ . To insure a safe operation when the fluids are used they selected a criteria requiring a  $V_2$  that is at least  $1.1 V_{s1g}$  compared to FAR 25 requirement of  $1.13 V_{s1g}$ . Reducing the margin to stall from 13% to 10% implies a corresponding lift loss of 5.24%. The algebraic analysis behind this reasoning is presented in Ref 2.

It should be noted that the 5.24% lift loss refers to the maximum lift coefficient for a three dimensional aircraft or wind tunnel model whereas the present study considers a two dimensional wing section at a  $C_l$  corresponding to  $V_2$ . Determining the correlation between the three dimensional wing maximum lift degradation and the two dimensional lift degradation at an angle of attack corresponding to speed  $V_2$  is considered to be beyond the scope of the present study. However the criteria for contamination effects will be assessed via the lift loss percentage, whatever the acceptable limit would be.

To find a satisfactory combination of angle of attack and lift coefficient both during ground roll and at speed  $V_2$ , several different slat and flap configurations were tested. Speed  $V_2$  was limited to 60 m/s by the wind tunnel practical maximum speed. After a set of extensive tests the best wing configuration appeared to be slats deflected  $11^\circ$  and flaps  $15^\circ$  which gave the following combination of angle of attack and lift coefficient:

- Ground roll (acceleration to 60 m/s)  $\alpha = 0^\circ$  and  $C_l = 0.51$
- Speed 60 m/s ( $V_2$ ) wing model rotated  $\alpha = 8^\circ$  and  $C_l = 1.28$

The analysis and reasoning behind these figures are described in detail in Ref. 7. This combination gave a realistic lift coefficient difference ( $\Delta C_l$ ) between take-off roll and flight at  $V_2$  and fairly realistic angles of attack. The primary objective was however the  $\Delta C_l$ .

The chosen speed-angle of attack ( $\alpha$ ) - time sequence for wind tunnel runs was as follows:

- At  $\alpha = 0$  wind tunnel speed was accelerated from idle speed to 60 m/s.
- As soon as the speed reached 60 m/s it was kept constant and the wing section was rotated at a rate of  $3.0^\circ/s$  to  $\alpha = 8^\circ$

- After rotation to  $\alpha = 8^\circ$  the angle of attack and wind tunnel speed were kept constant for 40 s.

The time used to accelerate the wind tunnel speed to 60 m/s is constant 30 s as per AAT<sup>1</sup> .

## 5. Previous test results

The previous wind tunnel tests by the author, presented in ref. 7, are summarized in chapters 5.1 to 5.3.

### 5.1 Clean wing aerodynamics

The attainable range of lift coefficients for the take-off simulation tests was a tradeoff between contradicting requirements. There was a need for a chord large enough to reach a reasonable Reynolds number. Also the slot dimensions for flaps and slats had to be large enough to get the fluids flowing without clogging. The restricting factor was the wind tunnel balance limit load (with a reasonable margin) for the lift force. This constrained the maximum lift coefficient during the tests to be below the ideal value.

For the same reason it was impossible to reach the stall with a rotation speed of 60 m/s. Stall with lower speeds would have led to incomparable Reynolds numbers. As the chord of the model was relatively large the stall situation was not considered to be risk free regarding the wind tunnel diffuser flow. The lift and moment coefficients for a clean wing model are presented in Fig. 2.

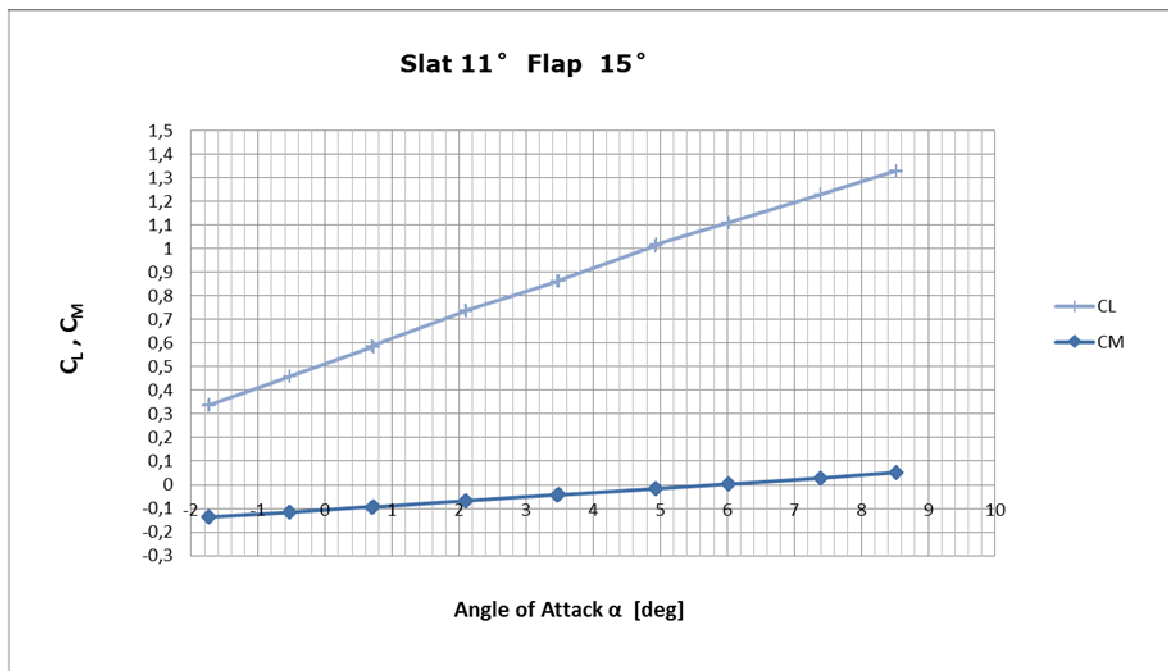


**Figure 2.** Lift and moment coefficient variation with  $\alpha$  at a speed of 60 m/s ( $Re\ 2.9\ 10^6$ ) for the wing model.

### 5.2 General Qualitative Observations

During the test runs video recordings were taken to analyze the wave formation and the fluid flow off. The flow off begins at the trailing edge somewhat earlier than in the one element model of Ref. 8 as there is airflow also in the slot between the flap and the wing main element. The first waves during the acceleration phase appeared near the mountings of the model probably due to the local flow acceleration around the fittings.

Most of the wing main section is clear of the fluid when the speed has reached 60 m/s just prior to the rotation (Fig. 3). However, there is still a clearly visible fluid layer at the trailing edge area. Within one second after the rotation a secondary flow wave appears from the lower side of the wing section through the slat gap. The secondary wave is visible in Fig. 4 at a 47-50 % chord position. In Fig. 5 there is a graphical presentation of the secondary wave movement in case of Type II fluid. The average speed (linear fit

in Fig. 5) of the secondary wave is 7.2 % of chord per second = 0.047 m/s. This means that the secondary wave reaches the trailing edge within about 10 s after rotation.

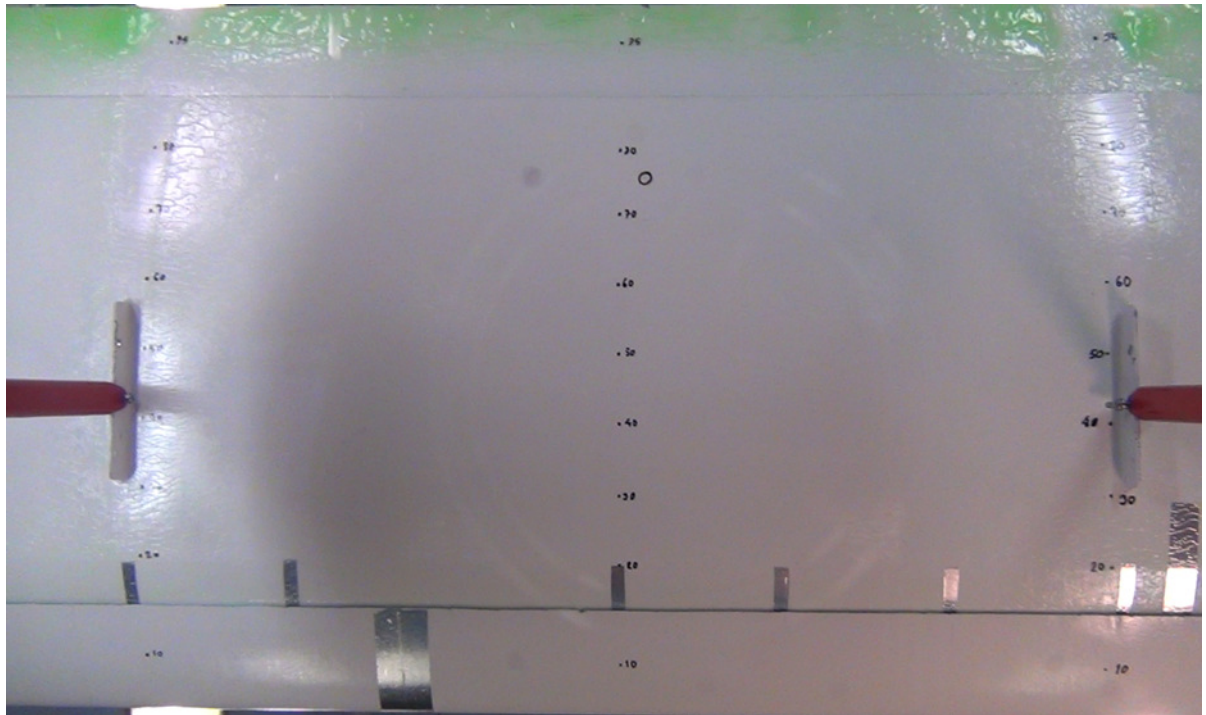


**Figure 3.** Fluid distribution just prior to rotation.

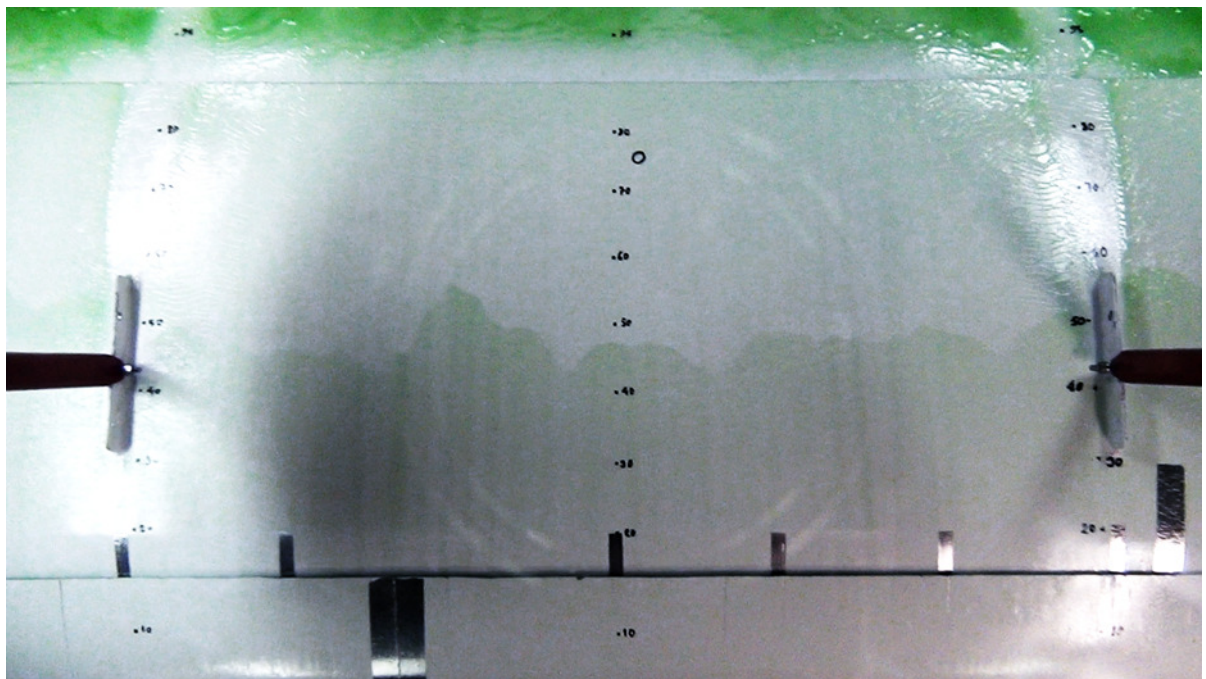


**Figure 4.** Secondary wave at a chord position of 47-50%.

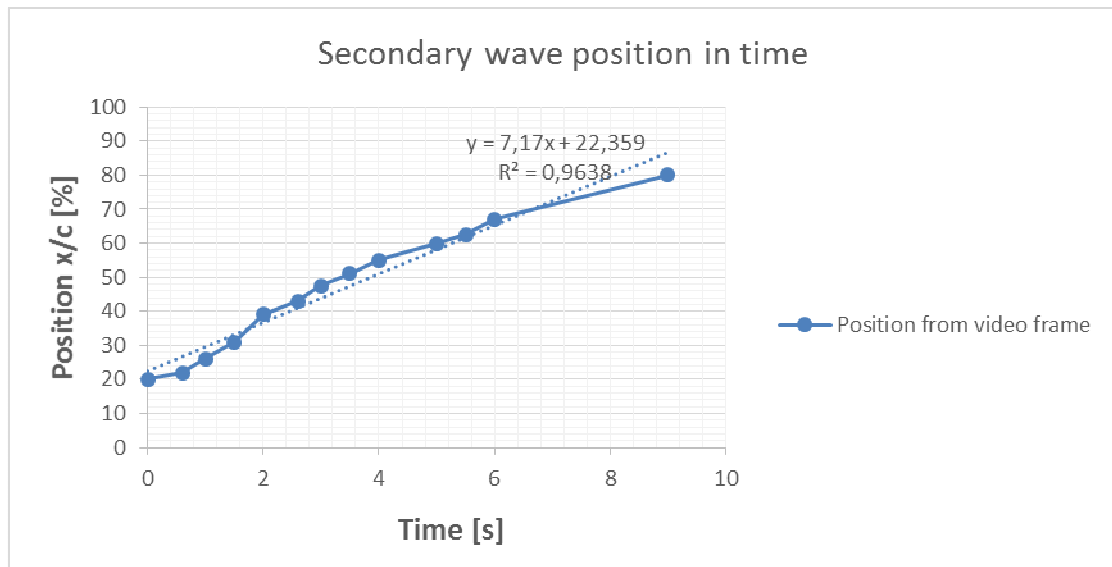


**Figure 5.** Secondary wave movement along the wing section chord. The dotted line is a linear fit of the measured curve. Time is measured from the point when the wing model has reached the angle of attack of  $\alpha=8^\circ$  after rotation

### 5.3 Lift Degradation Results

All together 7 different anti-icing treatment related parameters were studied in Ref 7. Prior to each test with anti-icing treatment the clean wing case was measured in Ref 7 to eliminate different daily changing factors on the results. As stated earlier the clean wing case was quite well repeatable. However, this was not the case after anti-icing treatment. The noise levels of measured lift coefficient after anti-icing treatment were clearly higher than for the clean wing case up to the end of each test run.

Along with the differences in the lift degradation results the similarities between all of the fluid tests in Ref 7 (20 different tests) open up some new aspects. The behavior of all fluid tests followed evidently a clear pattern as seen in Fig 6. The initial lift loss mean value of 6 % decreases down to 4 % within 10 first seconds after the rotation. The next 1.5 percentage point decrease to the value of 2.5 % takes an additional 25 seconds. The curve shows almost asymptotic behavior with relatively low and evenly distributed standard deviation (mean value of 0.52 percentage units). This result supports the conclusion that the secondary wave which was earlier observed to prevail on the upper surface for the 10 first seconds after the rotation may account for a significant part of the initial lift loss.

To study further the effect of the secondary wave on the lift degradation after rotation an additional test pair was designed. With the same anti-icing treatment a slats  $11^\circ$ , flaps  $15^\circ$  configuration and a configuration with slats and flaps retracted were compared with each other. In the case of slats and flaps retracted the slat gap was sealed. This test pair would then answer for two questions:

- will there appear a secondary wave on the wing section with slats and flaps retracted after the rotation – if not:
- what is the effect of secondary wave on the lift degradation

Naturally the answer for the second question is not straightforward as two different wing section configurations are compared. However if the difference is significant it supports the assumption that secondary wave has a significant effect on lift degradation in general.

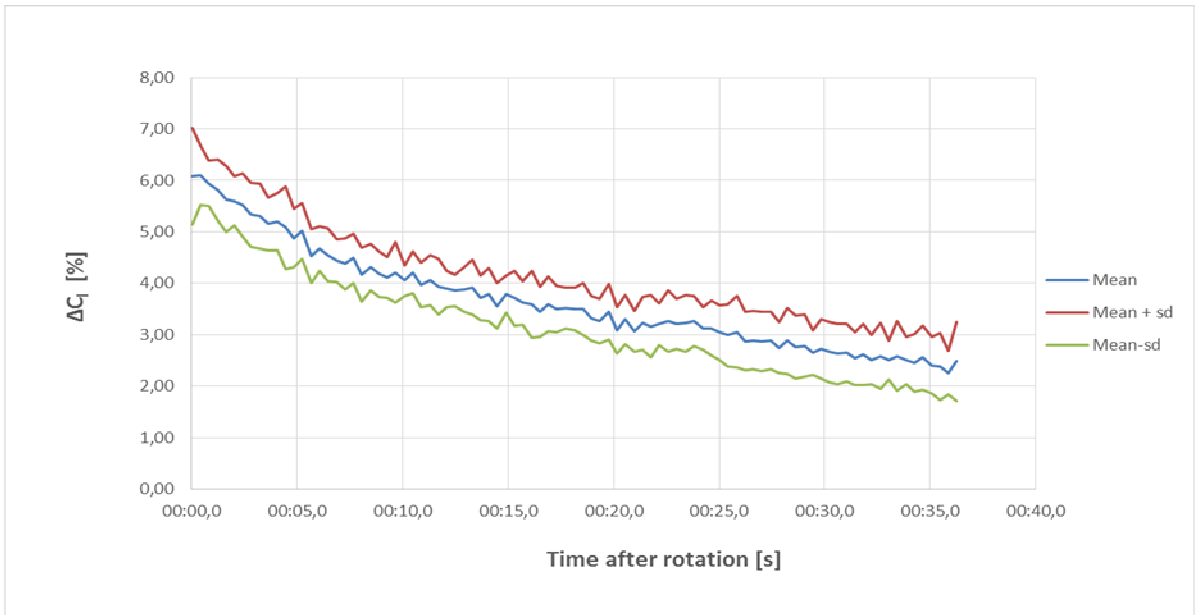


**Figure 6.** Mean lift degradation and its deviation in time for all fluid tests



## 6. Secondary wave tests

### 6.1 General Qualitative Observations

During the secondary wave tests the fluid movements were videotaped from two different directions: from the ceiling of the test section and through the test section Plexiglas door to get a view from the lower side of the wing section. The video recordings from the test section sealing confirmed that no secondary wave appeared on the wing section upper side when the slats and flaps were retracted and the slat gap sealed whereas on the slats  $11^\circ$ , flaps  $15^\circ$  configuration a secondary wave appeared just as during all the tests in Ref. 7, see Fig. 7. The trailing edge area in the configuration slats and flaps retracted seem to have more anti-ice fluid left due to the closed gap between the flap and the main element of the wing section.

To find out how the secondary wave is formed there were video recordings taken from below the model for both configurations. It was initially assumed that the cause of the secondary wave would be the shift of stagnation line towards the trailing edge after the rotation which then would have moved the fluid collected during the take-off roll phase around the wing section main element to the upper side. However the video tape shows clearly that when the slat is extended to  $11^\circ$  the lower stagnation line behind the slat is moving towards the leading edge instead of moving towards the trailing edge after the rotation.

What is seen before the rotation is that the fluid is moving during the whole take-off run phase towards the slat gap. It most probably is collected to the slat cove and be then depleted to the upper side after the rotation when the flow configuration in the slat gap changes. The positions and movement of the stagnation lines and flow direction before and after the rotation is shown in Figure 8. In the case of slats and flaps retracted configuration the stagnation line moves somewhat backwards as expected. However, the wing section nose area is clean of fluid at the point of rotation and there is not any fluid left for a secondary wave to build up, see Fig. 8 B and C.

As there was a secondary wave built up in the tests of Ref. 5 where the wing section was not equipped with a slat it is obvious that the mechanism for a secondary wave appearance changes from a wing section type to another. In Ref. 5 it is assumed that the buildup of the secondary wave is connected to the laminar separation bubble that forms to the sharp nosed wing section in question. However there is no photo or videotape material on the tests of Ref. 5.

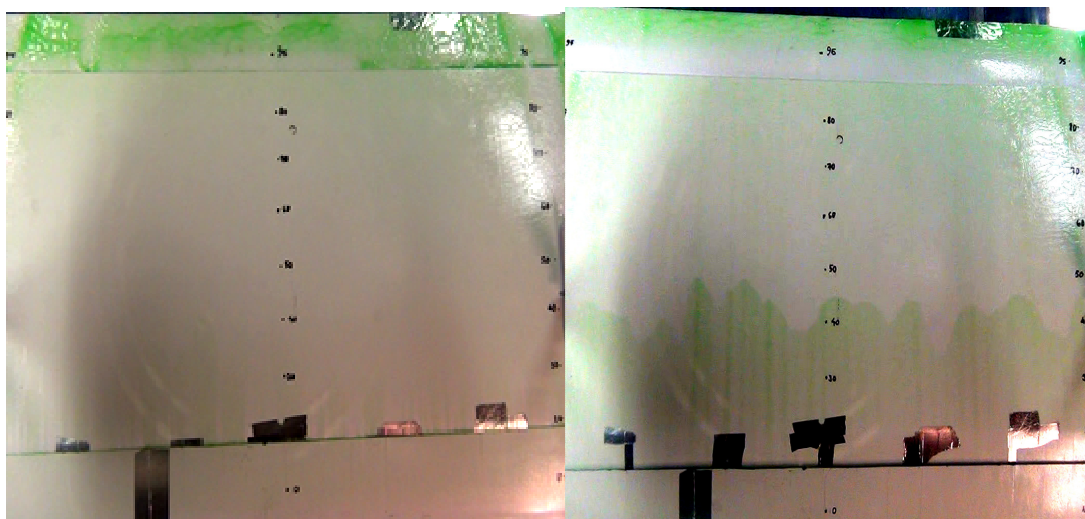
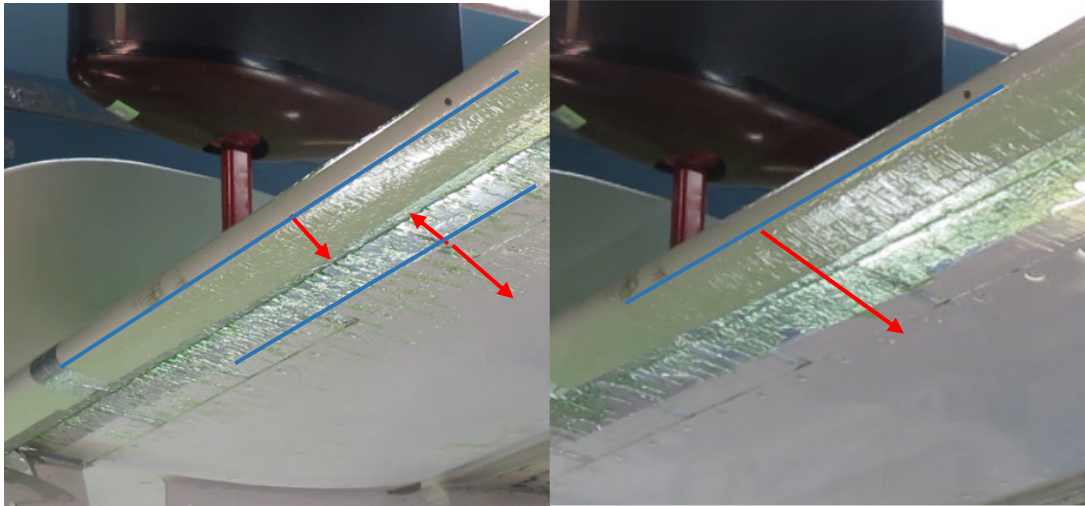
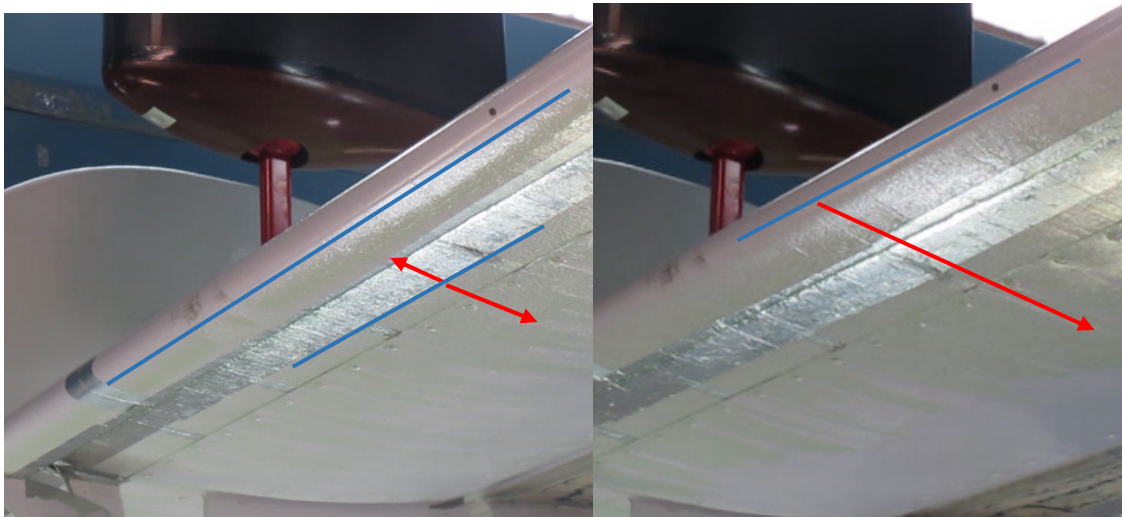


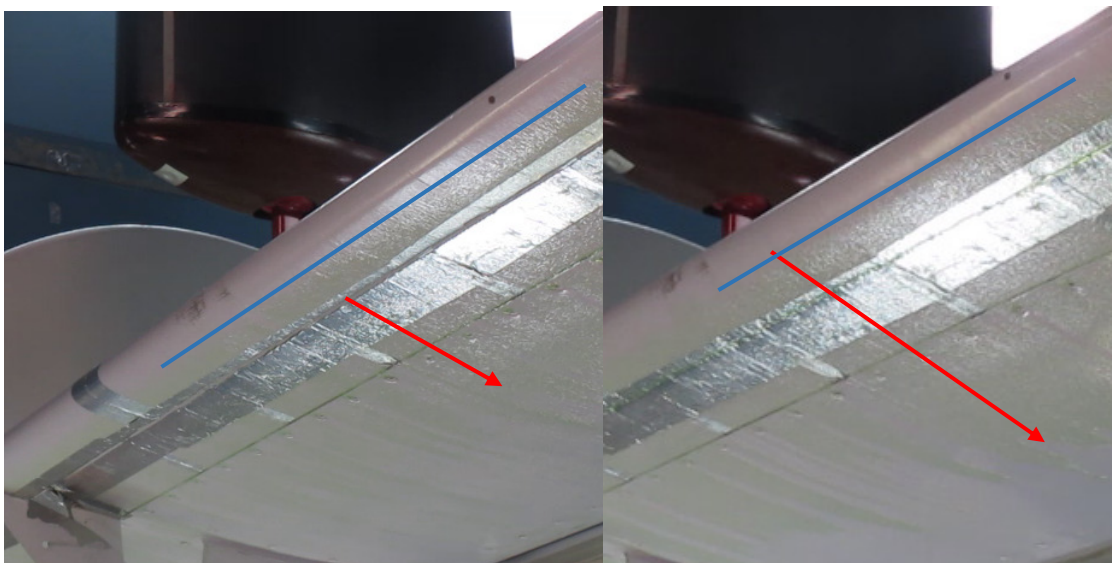
**Figure 7.** Slats, flaps retracted (left): no secondary wave. Slats  $11^\circ$ , flaps  $15^\circ$ : a clear secondary wave visible (right)



A. Wind tunnel speed 30 m/s



B. Wind tunnel speed 60 m/s just prior to rotation



C. Just after rotation

**Figure 8.** Flow directions (red arrows) and stagnation line (blue line) during the acceleration phase and after the rotation. Left figures: configuration slats  $11^\circ$  and flaps  $15^\circ$ , right figures: configuration slats and flaps retracted and slat gap sealed.



## 6.2 Lift degradation measurements

To estimate the contribution of the secondary wave to the lift degradation the lift loss due to the fluid application was measured for both configurations – slats and flaps retracted and extended. In both cases the fluid applied was Type IV. The results are presented in Fig. 9. There are the mean values (+/- standard deviation) of measurements in Ref. 7 plotted in the background of Fig. 9 as for reference. The lift loss of the configuration, with the slats and flaps retracted, begins immediately after rotation approximately with a value that the lift loss of the configuration, with slats  $11^\circ$  and flaps  $15^\circ$ , ends with 30 seconds after rotation.

As the different configurations represent two different wing sections the comparison between the results is not straightforward. However, as the difference between the two configurations is so remarkable it supports the assumption that a secondary wave has a considerable contribution to the lift degradation after rotation.

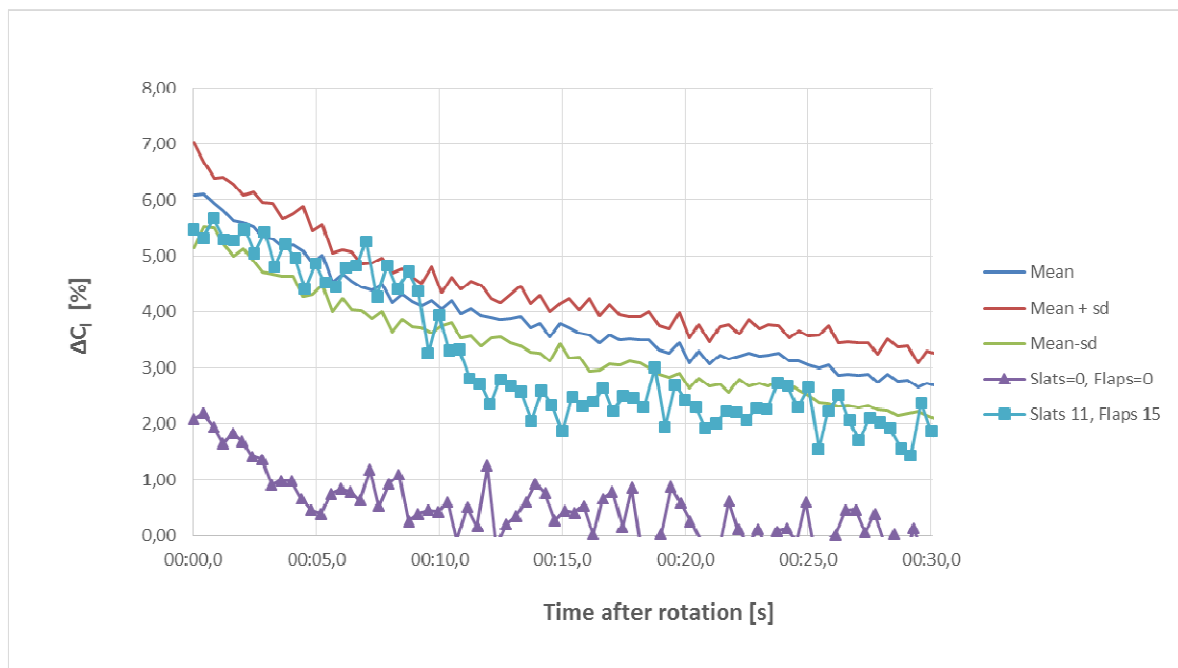


**Figure 9.** Lift degradation after rotation for configurations slats  $11^\circ$ , flaps  $15^\circ$  and slats, flaps retracted. All the lift degradation measurements of Ref. 7 are plotted in the background (Mean +/-sd)

## **7. Conclusions**

The main findings of this study were:

- The emerging mechanism of a secondary wave depends on wing section geometry and configuration
- On DLR-F15 wing section the secondary wave forms from the fluid that is collected to the slot gap area. This fluid depletes onto the upper side of wing section after the rotation when the flow configuration between the slat and wing section main element changes
- For a DLR-F15 wing section in configuration where slat and flaps are retracted no secondary wave appears on the upper side of the wing section after the rotation
- The secondary wave is probably responsible for most of the lift degradation after rotation.

This study may be considered as a motivation for further research on this topic and the following issues should be addressed in the future:

- The differences in emerging mechanisms of secondary wave in different wing section geometries and configurations to understand the interrelationship between the wing section pressure distribution and buildup of secondary wave.
- Determining the thickness of the secondary wave from the video tapes of present study using the analysis method developed in Ref. 8. This would enable to assess better the contribution of secondary wave on the lift degradation

## 8. References

1. "Standard Test Method for Aerodynamic Acceptance of SAE AMS 1424 and SAE AMS 1428 Aircraft Deicing/ Anti-icing Fluids", AS5900 Rev.B, SAE International, 26 July 2007.
2. Broeren, A., Riley, J: "Review of the Aerodynamic Acceptance Test and Application to Anti-icing Fluids Testing in the NRC Propulsion and Icing Wind Tunnel" NASA TM 2012-216014, Aug. 2012
3. Hill, E.G., and Ziertzen, T.A., "Aerodynamic Effects of Aircraft Ground Deicing /Anti - Icing Fluids," Journal of Aircraft, Vol. 30, No. 1, Jan. -Feb., 1993
4. Runyan, L.J., Ziertzen, T.A., Hill, E.G., Addy, H.E., "Lewis Icing Research Tunnel Test of the Aerodynamic Effects of Aircraft Ground Deicing/Anti-icing Fluids", NASA-TP 3238, 1992
5. Broeren A., Lee S., Clark C., "Aerodynamic Characterization of a Thin, High Performance Airfoil for Use in Ground Fluids Testing", AIAA 2013-2933, 5th atmospheric and Environments Conference, June 24-27. 2013, San Diego CA.
6. Wild, J.: "Experimental investigation of Mach- and Reynolds-number dependencies of the stall behavior of 2-element and 3- element high-lift wing sections", AIAA 2012-0108, 50th AIAA Aerospace Sciences Meeting including the New Horizons Forum and Aerospace Exposition 09 - 12 January 2012, Nashville, Tennessee
7. Koivisto, P. "Effects of Anti-icing Treatment on Lift Degradation during Simulated Take-off" Trafi Publications 25/2013.
8. Koivisto, P. "Anti-icing Fluid Flow off on a Wing Section During Simulated Taxi and Take-off", AIAA 2013-2932, 5th atmospheric and Environments Conference, June 24-27. 2013, San Diego CA.